Nanoscale

PAPER

View Article Online
View Journal | View Issue

Cite this: *Nanoscale*, 2015, **7**, 8619

Ultrasensitive SERS detection of trinitrotoluene through capillarity-constructed reversible hot spots based on ZnO–Ag nanorod hybrids†

Xuan He,*[a] Hui Wang,[a] Zhongbo Li,*[b] Dong Chen,[a] Jiahui Liu[a] and Qi Zhang*[a]

Received 29th December 2014,
Accepted 1st April 2015

DOI: 10.1039/c4nr07655a

www.rsc.org/nanoscale

A simple and efficient self-approach strategy was used to apply ultrasensitivity and self-revive ZnO–Ag hybrid surface-enhanced Raman scattering (SERS) sensors for the highly sensitive and selective detection of explosive TNT in both solution and vapour conditions. The good ultrasensitive sensing performance is a result of the abundant Raman hot spots, which were spontaneously formed in a reversible way by the self-approaching of flexible ZnO–Ag hybrid nanorods driven by the capillary force of solvent evaporation. Moreover, the enhancement effect was repeatedly renewed by the reconstruction of molecular bridges, which could selectively detect TNT with a lower limit of 4×10^{-14} M. In addition, TNT vapor was also tested under this sensor, whereby once the ZnO–Ag NRs hybrid substrate was dipped in TNT, this substrate could detect the existence of TNT even in 5 detection cycles *via* a capillarity-constructed reversible hot spots approach. Compared with other pure Ag-based SERS sensors, this ZnO–Ag hybrid SERS sensor could rapidly self-revive SERS-activity by simple UV light irradiation and could retain stable SERS sensitivity for one month when used for TNT detection. This stable and ultrasensitive SERS substrate demonstrates a new route to eliminate the oxidized inactive problem of traditional Ag-based SERS substrates and suggests promising use in the applications of such hybrids as real-time online sensors for explosives detection.

Introduction

Since the discovery that Raman signals could be enhanced at a rough silver electrode, surface-enhanced Raman scattering (SERS) has been a subject of interest in research for both understanding the enhancement mechanism and for chemosensing purposes.[1] Many studies have demonstrated that nanogaps between the metal nanostructures are required to generate the "hot spots" typically associated with high SERS activity.[2] However, nanoscale control on the interspace between two nano-building-blocks of the SERS-substrate faces problems such as structural reproducibility, complex processes and high cost.[3] A recent review by Liz-Marźan and Polavarapu provided a detailed overview of a type of flexible substrate useful for nanoplasmonic sensing, which could provide a new prospect to overcome these problems.[4] These substrates often construct "hot spots" by the self-conglutination of nanorods to trap molecules among the nanorods by utilizing electronic,[5] ferroelectric,[6] thermal[7] or mechanical strain[8] effects. However, with most of the effects, the constructed "hot spots" in the SERS-active nanostructures are not reversible, and therefore the sensor can be used only once. Moreover, it is still an intriguing challenge to create reversible hot spots and to trap target molecules for practical plasmonic sensing purposes.

Recently, a few brilliant reports have indicated that silver (Ag) nanotube or nanorod arrays could construct reversible Raman hot spots with outstanding enhancement ability through the capillary force of a solvent evaporation strategy.[9] Unfortunately, Ag nanostructures are easily oxidized in air, resulting in a loss of the hot spots and inactivation of the SERS substrates. In addition to the reversible, ultrahigh activity of SERS substrates, the stability of SERS substrates is often a major concern from the viewpoint of practical applications.[10] Nowadays, hybrid nanostructures, such as ZnO/Ag and TiO_2/Ag, have attracted considerable attention because of their unique shape-composition-dependent properties and multiple functionalities that are rarely achievable in single-component nanostructures.[3d,11] The stability problem of Ag-based SERS substrate could be solved by the development of functional Ag-hybrid composite nanostructures as SERS substrates.[12] Moreover, the design of a stable Ag-hybrid substrate that could

[a]*Institute of Chemical Materials, China Academy of Engineering Physics, Mianyang 621900, China. E-mail: xuan.hellen@gmail.com, jackzhang531@gmail.com*
[b]*Key Laboratory of Materials Physics, Anhui, Key Laboratory of Nanomaterials and Nanostructures, Institute of Solid State Physics, Chinese Academy of Sciences, Hefei, 230031, China. E-mail: sdlzb@issp.ac.cn*
†Electronic supplementary information (ESI) available. See DOI: 10.1039/c4nr07655a

create reversible hot spots by a capillary force effect could be applied to SERS practical detection.

Referring to real SERS application, as the Raman spectrum originates from vibrations in the chemical bonds of the analyte, any chemical species can, in theory, be analyzed. For this reason, SERS has shown great potential to become a versatile analytical tool for both chemical and biochemical sensors in liquid and gas phases.[13] Furthermore, SERS has been named as a very promising method for explosives sensing, with fast analysis speed and high sensitivity being the main advantages.[14] Among all explosives, the detection of illegally transported explosive materials, such as 2,4,6-trinitrotoluene (TNT), is very important for various fields, including humanitarian demining, remediation of explosives waste sites, homeland security, and forensic applications.[15,16] Many reports have demonstrated that SERS substrates based on hybrid nanostructures can be repeatedly used to detect TNT.[17,18] However, such impressive SERS face problems with the stability and reproducibility of the Raman signal.

In this paper, we report for the first time, the development of large-scale nanorod-shaped ZnO–Ag hybrid SERS substrates for the highly sensitive, selective, and stable detection of explosive TNT with a lower limit of 4×10^{-14} M. As shown in Scheme 1, utilizing a directional growth design method, we obtained vertical ZnO nanorods (NRs) with a [0001] growth direction. These long ZnO NRs showed excellent flexibility and were much easier to self-approach when driven by an external effect, *e.g.* by capillarity. Next, Ag nanoparticles (NPs) were decorated onto the surface of the ZnO NRs to fabricate ZnO–Ag hybrids as SERS substrates. Thus, high density hot spots could be formed in a reversible way *via* the self-approaching of ZnO–Ag NRs driven by the capillary force of the solvent evaporation. Once the TNT molecules were captured *via* the formation of a charge-transfer *p*,*p*′-dimercaptoazobenzene (DMAB)-TNT-DMAB bridge on the flexible ZnO–Ag NR array hybrids and trapped in hot spots, high enhancement Raman intensity could be achieved. A vapor of TNT was also collected under this 4-ATP-modified SERS substrate. Then, by repeating the addition of ethanol four times and the detection for five cycles with the parallel Raman intensity of 4-ATP, the cycle experiments showed that TNT could be persistently detected using the hot spots created by this solvent evaporation inspired method. Furthermore, compared with other single-component Ag-based SERS sensors, this ZnO–Ag hybrid SERS sensor could rapidly revive the hot spots of SERS-inactive sensors by simple UV light irradiation, and these could then maintain stable SERS-active ability for one month. The application of this stable and ultrasensitive SERS substrate would be essential for the practical identification of explosives and for monitoring.

Results and discussion

The as-prepared ZnO NRs on the substrate with different lengths prepared *via* the simple hydrothermal method[19] are shown in the ESI (Fig. 1 and S1†) and were characterized by field-emission scanning electron microscopy (FE-SEM). The side-view SEM images reveal that the average length of the ZnO NRs was ~550 nm, 960 nm and 1.5 μm with the reaction times of 3 h, 8 h and 12 h, respectively (for 1.5 μm length ZnO NRs, see Fig. 1(a)–(c) and for other length ZnO NRs, see Fig. S1 in the ESI†). Moreover, the transmission electron microscopy (TEM) images further confirmed that the hybrid ZnO NRs was ~35 nm in diameter (Fig. 1d). Ion sputtering was then per-

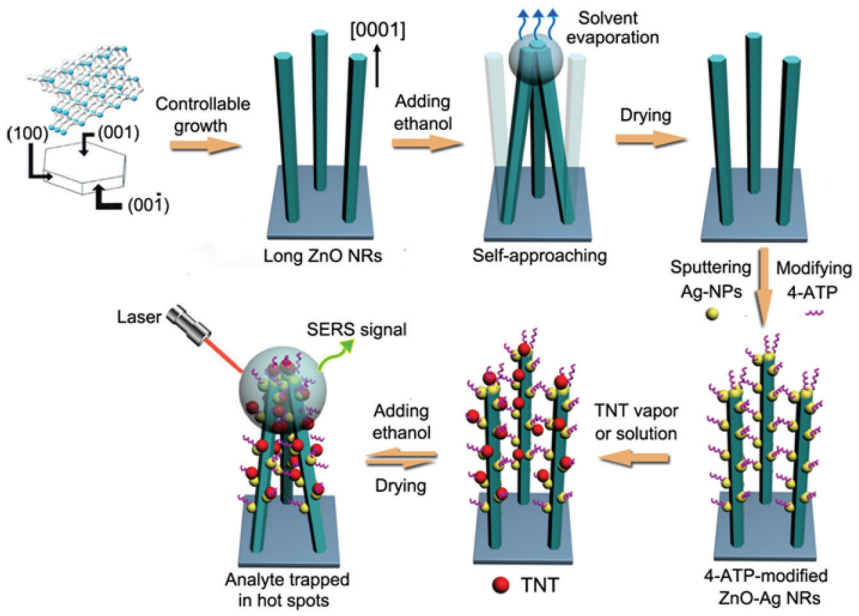

Scheme 1 Schematic of the self-approaching of NRs driven by the capillary force of solvent evaporation.

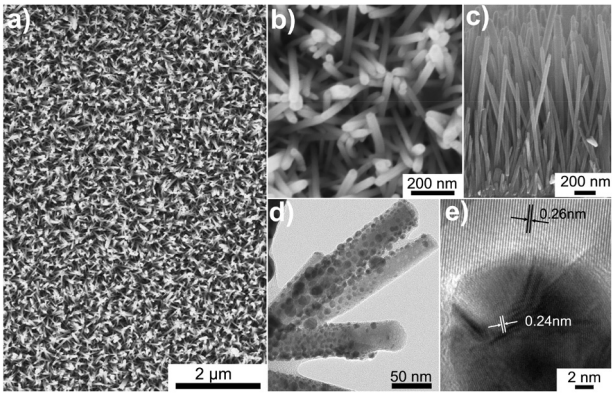

Fig. 1 (a) SEM image of ZnO NRs; (b) enlarged FE-SEM image of ZnO NRs; (c) side-view FE-SEM image of ZnO NRs; (d) TEM image of the as-presented ZnO–Ag samples; (e) HRTEM image of the as-presented ZnO–Ag samples of (d).

formed to assemble the Ag NPs onto the ZnO NRs with different deposition times (4 min, 10 min, 16 min, and 26 min, see Fig. S2†). High-resolution TEM (HR-TEM) images (Fig. 1e) displayed the clear lattice fringes of ZnO and Ag and revealed the single-crystalline nature of ZnO. Among these, the measured lattice spacing was about 0.26 nm, which corresponds to the (0002) lattice plane of wurtzite ZnO,[20] whereas the lattice spacing of 0.24 nm matched with the fcc Ag (111) plane, which agree well with the XRD results (Fig. S3–S4†).

In order to evaluate the SERS performance of the ZnO–Ag hybrids substrate, the ZnO NRs with different length were sputtered on Ag nanoparticles for different durations. Raman measurements demonstrated that 1.5 μm length ZnO nanorod arrays with 16 min Ag-sputtering showed the highest SERS activity (Fig. S5†). When 1×10^{-14} M R6G ethanol was directly added onto the hybrid arrays with the length of 1.5 μm, the Raman signals of R6G could clearly be detected after ~65 s (Fig. S6–S8†). The SERS enhancement factors (EF) for R6G on the ZnO–Ag NRs were calculated according to the equation $EF = (I_{SERS}/I_{bulk})(N_{bulk}/N_{surface})$, where I_{SERS} and I_{bulk} were the peak intensities of 10^{-11} M R6G on the ZnO–Ag NRs substrate and 1×10^{-3} M R6G on a silicon substrate at 611 cm^{-1}, respectively. N_{SERS} and N_{bulk} were the number of R6G molecules excited by the laser beam on the ZnO–Ag NRs hybrid substrate and Si substrate, respectively. Moreover, the SERS enhancement factors (EF) for R6G on the ZnO–Ag NRs were calculated to be about 4.3×10^{8} after ~65 s (see ESI Fig. S6–S8†).[21] This huge enhancement was due to the formation of Raman hot spots through the self-approaching of flexible ZnO–Ag NRs driven by the capillary force from the solvent evaporation (Scheme 1). Correspondingly, other hybrid arrays with lengths of 960 nm and 550 nm exhibited much lower, or even no enhancement, under the same condition (Fig. S9–S10†). This clearly indicates that the longer ZnO NRs benefited self-approaching and thus the formation of many more Raman hot spots with the help of the capillary force from solvent evaporation due to their better flexibility.

Subsequently, different solvents were used for the observation of the capillary forces from the solvent evaporation, namely, ethanol, water, acetone, methyl alcohol, isopropanol and ethyl acetate. First, ZnO–Ag NRs hybrids were further modified with 4-ATP through the formation of Ag–S bonds by immersing the hybrids in a very dilute 4-ATP alcohol solution (1×10^{-9} M). The Raman signal of the 4-ATP molecules was very faint due to the extremely low number of molecules at these dry arrays. If a droplet of 5 μL ethanol was added onto identical NR arrays, ethanol could completely permeate into the interspaces of the top-closed NRs (inset of Fig. 2a) and the Raman spectra were recorded, as shown in Fig. 2a. Interestingly, with the evaporation of ethanol, the enhanced Raman signals of 4-ATP gradually appeared after ~25 s and achieved the strongest value at ~65 s (Fig. 2a). Furthermore, the enhanced signals maintained the equivalent intensity for a

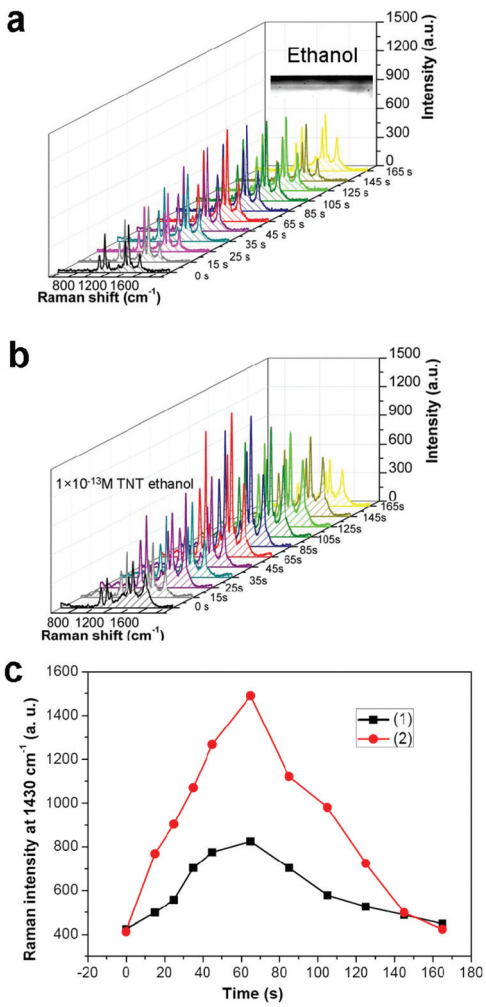

Fig. 2 (a) The time-resolved Raman spectra of 4-ATP after dropping in 5 μL ethanol. The inset in part (a) is the image of ethanol droplets on the substrate; (b) 1×10^{-13} M TNT alcohol solution on the 4-ATP modified ZnO–Ag hybrid NR arrays; (c) line (1): the temporal evolution of the corresponding Raman intensity at 1430 cm^{-1} of (a); line (2): the temporal evolution of the corresponding Raman intensity at 1430 cm^{-1} of (b).

definite time from ~85 s to 125 s before finally disappearing after the evaporation finished. These temporal spectral evolutions confirmed that the capillary force from the ethanol evaporation induced the self-approaching of the ZnO–Ag NRs hybrids to form the hot spots, making the Raman signals of 4-ATP well detectable. Moreover, a same volume droplet of other solvents, such as acetone, methyl alcohol, isopropanol, ethyl acetate and ultrapure water, was also added onto the dry ZnO–Ag NR hybrids (Fig. S11–S15†). The solvent volatilization speed of acetone and methyl alcohol was much higher than that of ethanol. Therefore, the best scan-time was hard to confirm before the solvent volatilization process finished (Fig. S11–12†). There were much lower Raman signals of 4-ATP observed with the increase in the observed time using isopropanol, ethyl acetate, and water as solvents due to the slow volatilization rate (Fig. S13–S15†). In addition, the measurement of the contact angle revealed a highly hydrophobic feature of the NR arrays for water (inset microscopic image of Fig. S15†). In contrast, other solvents could completely permeate into the interspaces of the ZnO–Ag NRs hybrids (inset of Fig. S11–S14†). Considering the factors of the solvent evaporation rate and the surface tension of the different solvents, the collection time and the enhancement intensity of the Raman peaks, ethanol was considered the most suitable solvent for the formation of capillarity-constructed reversible SERS hot spots during molecule detection.

In addition, the stability of the ZnO–Ag NRs hybrid SERS substrates was evaluated using 1.5 μm ZnO–Ag hybrids combined with ethanol as the solvent. All the R6G Raman spectra were obtained from 15 random points on the same piece of SERS substrate. The similar Raman spectra demonstrate the good signal reproducibility of this composite structure. Moreover, the relative standard deviation (RSD) of the major R6G characteristic SERS peaks was calculated to evaluate the reproducibility of the SERS signals, as shown in Fig. S16 and S17,† which reveal almost the same intensity for each characteristic band of R6G. The maximal RSD value of the signal intensities of the major SERS peaks was observed to be below 0.25, indicating that the ZnO–Ag NRs hybrid SERS substrates had a good reproducibility across the entire area. The experimental results suggest that the flexible ZnO–Ag NRs could be used as highly sensitive, reproducible and reliable substrates for Raman practical applications.

Inspired by the huge SERS performance induced by the capillary force from the solvent evaporation, the next goal was to explore potential applications in practical molecule detection. When 1×10^{-13} M TNT alcohol solution was added to the 1.5 μm ZnO–Ag hybrids, it was surprising that the Raman signals of 4-ATP were violently enhanced (Fig. 2b). The strongest signal intensity at 1430 cm^{-1} after ~45 s was ~3.55 times stronger than that obtained by the addition of pure ethanol (Fig. 2c). This was because the π–π conjugated structures between the TNT and 4-ATP could effectively promote the electronic transfer, leading to the enhanced Raman signals by a chemical mechanism (CM) enhancement (Fig. S18–19†).[18,21] Similarly, the Raman signals of 4-ATP gradually disappeared when the evaporation of solvent was completed. Based on the abovementioned results, the best measuring conditions for the detection of TNT were thus set at the volume of a 5 μL analyte droplet, with data recorded at ~65 s after the addition of the liquid droplet, and using a 5 mW and 2 μm laser beam. The Raman spectra of 4-ATP-functionalized ZnO–Ag hybrids in the presence of TNT at different concentrations were recorded (Fig. 3a). The error bar line is shown in Fig. 3b, wherein it can be seen that the Raman intensity of PABT obviously increased with the TNT concentration from 100 fM to 0.1 μM and exhibited a correlation coefficient $R = 0.9913$ in the range from 100 fM to 10 pM. Even in the case of 40 fM TNT, the Raman signal of PABT was 1.26-fold stronger than that by the addition of blank ethanol, and thus a detection limit of 4×10^{-14} M TNT was reached (Fig. S20–21†).

Then, the Raman spectra were obtained from TNT in the gas phase in the following manner.[22] An identical ZnO–Ag hybrid NR array SERS substrate was placed at the outlet of the pipe for 3 min wherein a Raman spectrum was recorded. Then, a 5 μL droplet of ethanol was added onto this hybrid SERS substrate, and a clear enhancement of the Raman spectra from a gradual increase to a gradual decrease was again observed, wherein the strongest signal intensity at 1430 cm^{-1} after ~45 s was ~7-times stronger than that from the pure 4-ATP Raman intensity in the same condition. The enhancement of the 4-ATP Raman spectra was completely attributed to the contribution of ultratraces of TNT in solution

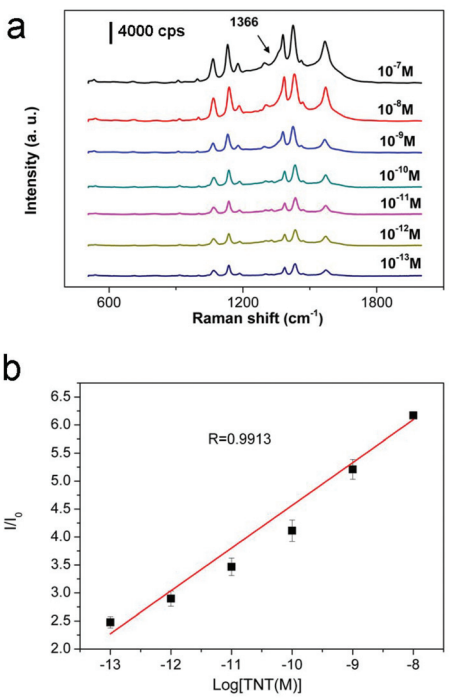

Fig. 3 (a) Raman responses of 4-ATP-functionalized ZnO–Ag hybrids in the presence of TNT at different concentrations: 1×10^{-7} to 1×10^{-13} M; (b) the corresponding calibration curve for SERS intensity *versus* −log[TNT], in which the SERS intensities were recorded at 1430 cm^{-1}.

or in the gas phase. After the substrate drying, we repeated the addition of ethanol 4 times and recorded the Raman spectrum for 5 cycles. As shown in Fig. 4, it is clear that the ZnO–Ag NRs are driven through the capillary force of solvent evaporation and formation highly SERS activity. Once the ZnO–Ag NRs hybrid substrate was enriched of TNT, this substrate could be used to inform the existence of TNT, even in 5 detection cycles through a capillarity-constructed reversible hot spots approach. These measurements strongly demonstrated that 4-ATP-modified ZnO–Ag NRs hybrids could be used as a promising SERS platform for sensitive TNT detection.

On the platform of 4-ATP-modified ZnO–Ag NRs hybrids, the mechanism for the TNT-induced resonance Raman enhancement of 4-ATP is proposed. As shown in Scheme 1, once the NR hybrids were exposed to ethanol, the ZnO NRs lean to form hot spots with the analyte molecules trapped between the top-closed NRs as the solvent evaporates from the arrays. The number of formed hot spots make it very likely that the TNT molecules would be located in a large number of hot spots giving rise to a large average Raman signal. Moreover, the π–π conjugated structures between TNT and 4-ATP could enhance the Raman signals by a chemical mechanism (CM) enhancement (Fig. S18–19†).[18,21] Thus, the enhancement of the 4-ATP Raman signals mainly originates from the resonances of the molecular bridge with both incident laser and surface plasma, with the aid of Raman hot spots formed by the self-approaching of the long flexile NRs hybrids. To further ascertain the recognition selectivity of the 4-ATP-modified ZnO–Ag platform, we prepared other structurally similar nitrated-explosive detection systems (10^{-9} M in ethanol) such as picric acid (PA), 2-nitrotoluene (NT), and *m*-dinitrobenzene (DNB), and 2,4-dinitrotoluene (DNT) (Fig. 5 and Fig. S22†). It could be seen that compared with TNT, weaker Raman enhancements were observed for PA, DNT, DNB, and NT. In addition, the peak intensity at 1430 cm^{-1} was about 7.86 times stronger than that obtained without TNT (Fig. 5a). However, other explosives were less than 2.5-times enhanced when acting with 4-ATP under the same conditions. Moreover, the UV-vis spectrum did not show any visible absorption when DNB, DNT, PA, and NT were mixed with 4-ATP in solution, suggesting that DNB, DNT, PA, and NT could not likely form an effective charge-transfer complexing chromophore with 4-ATP (Fig. 5b). All these experiments indicated that the 4-ATP-functionalized ZnO–Ag NRs hybrids provide an effective SERS platform

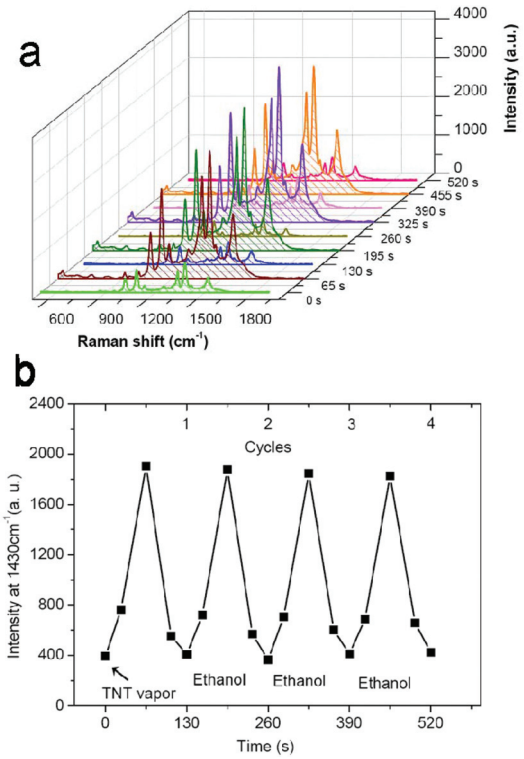

Fig. 4 (a) Cyclic detection of 4-ATP Raman intensity at 1430 cm^{-1} after the collection of TNT vapor for 3 min. A 5 μL droplet of pure ethanol was added onto this ZnO–Ag NRs hybrid SERS substrate before the Raman spectrum was recorded. After the drying of TNT ethanol, a 5 μL droplet of pure ethanol was added on the substrate and detected. (b) The temporal evolution of the corresponding Raman intensity at 1430 cm^{-1} of (a).

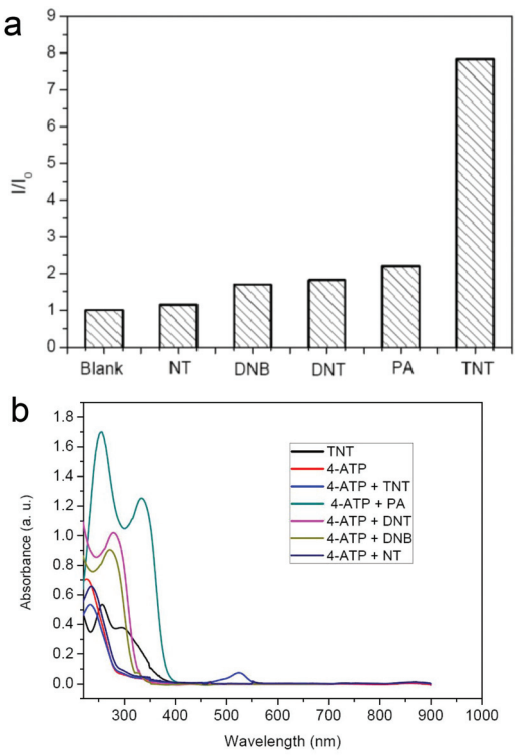

Fig. 5 (a) Comparison of the SERS intensity (1430 cm^{-1}) of different explosives with the same concentration of 10^{-9} M in ethanol, (*I* is the SERS intensity of 4-ATP interacting with explosives, and I_0 is the SERS intensity of 4-ATP); (b) UV-vis absorption spectra of TNT, 4-ATP, TNT and 4-ATP complex, PA and 4-ATP complex, DNT and 4-ATP complex, DNB and 4-ATP complex, NT and 4-ATP complex. The UV-vis spectra in solution were obtained using ethanol with a pH of about 6.94 as the solvent at room temperature with a path-length of 1 cm.

for TNT detection with good sensitivity, reproducibility, and selectivity.

As we all know, Ag is widely recognized as one of the best surface enhanced Raman active materials. However, the Ag-based nanomaterials would be easily oxidized gradually in air, as oxygen molecules could be absorbed onto the substrate surface and would then capture electrons from the Ag atoms, leading to the oxidation of the surface Ag atoms to Ag+ ions. This would result in a loss of the hot spots and inactivation of the SERS substrate, as a layer of silver oxide would form on the surfaces of these Ag nanomaterials (Scheme S1†). Hence, this was the most important reason why the use of Ag materials has been limited in practical applications.[18] As a result, the reactivation of such an inactive substrate would be essential for practical SERS detection applications. Consequently, a hybrid substrate that was kept in the dark in air for a month was examined. It first yielded poor SERS signals (Fig. 6a). However, when the substrate was irradiated with UV light, the ZnO NRs could absorb light in a particular region, and the excited electrons were eventually absorbed by the surface Ag+ ions, thereby reducing the Ag+ ions to Ag atoms and reactivating the SERS inactive Ag-decorated ZnO substrate. It was clearly demonstrated that UV light irradiation could effectively and rapidly revive the hot spots of the SERS-inactive Ag-decorated ZnO substrate.[18] To evaluate the reproducibility of the self-reviving substrates, five substrates made from different batches were kept in the dark in air for a month, and then revived under UV light and used as substrates to examine TNT (10^{-12} M) for comparison (Fig. 6, Fig. S23†). The average deviation of the peak height of the self-reviving substrates at 1430 cm^{-1} was 6.27%. In addition to the good self-reviving reproducibility, the five substrates displayed stable and high SERS enhancements in TNT detection. As shown in Fig. S24,† the distinct bands could be still easily identified in the Raman spectra even at the low concentration of 10^{-12} M by the five self-revived substrates after 1 month. Moreover, different self-reviving substrates were used for R6G, 4-ATP and TNT detection (Fig. S23–S29†). It should be noted that neither a shift in the major Raman peaks nor a significant change in the Raman intensity occurred in the SERS spectra from the substrate placed in the dark cabinet for 30 days, revealing that the as-prepared substrate was stable for at least a 30-day period. This long-term stability in the dark is of great importance for handling and storing the SERS-active substrates in practical applications.

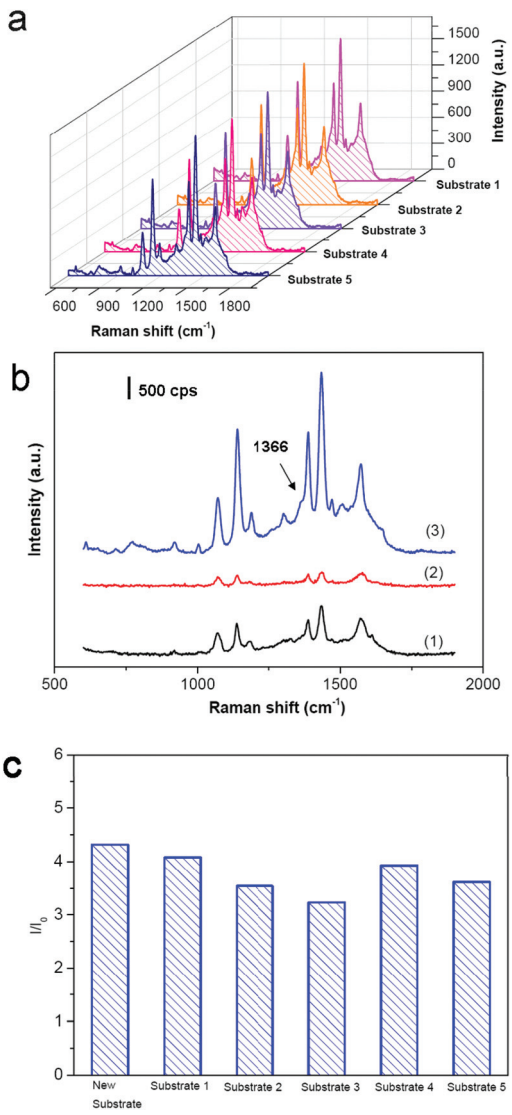

Fig. 6 (a) SERS spectra of self-reviving substrates to detect TNT (1×10^{-12} M). The integration time is 5 s; (b) curve (1) the as-prepared ZnO–Ag NRs hybrid substrate 1 of SERS spectra of probe 4-ATP; curve (2) kept substrate 1 in dark air for a month; curve (3) after irradiating with UV light for 5 min for the substrate 1 in curve (2), then used this self-reviving substrate 1 to detect TNT (10^{-12} M) in ethanol. The integration time was 5 s; (c) comparison of the SERS intensity (1430 cm^{-1}) of five self-revive substrate and new as-prepared substrate with the same TNT detection condition of 10^{-12} M in ethanol. (I was SERS intensity of 4-ATP interacted with TNT, and I_0 was SERS intensity of 4-ATP).

Conclusion

In this paper, we reported for the first time the application of self-reviving SERS-active NR-shaped ZnO–Ag hybrid SERS substrates for the highly sensitive and selective detection of explosive TNT by a simple and efficient self-approaching strategy. During the detection, the self-approaching of the ZnO–Ag hybrids driven by the capillary force of solvent evaporation could efficiently and spontaneously induce the formation of reversible Raman hot spots. In contrast with other Ag-based SERS sensors, this SERS sensor could rapidly revive the hot spots of the SERS-inactive sensors by simple UV light irradiation and could retain a stable SERS-active ability for 1 month. Furthermore, the SERS substrate could be employed for both liquid and gas phase TNT detection. The stable and ultrasensitive SERS substrate demonstrates a new route to eliminate the oxidized inactive problem of traditional Ag-based SERS substrates and suggests promising use in the applications of such hybrids as real-time online sensors for

explosives detection. Further studies on the exploitation of other substrates for SERS applications are underway.

Acknowledgements

This study was supported by the National Natural Science Foundation (no. 21302176), the China Postdoctoral Science Foundation (no. 2014M561843) and the Development Foundation of CAEP (no. 2013B0302042).

Notes and references

1 (*a*) R. S. Golightly, W. E. Doering and M. J. Natan, *ACS Nano*, 2009, **3**, 2859–2869; (*b*) J. Homola, *Chem. Rev.*, 2008, **108**, 462–493; (*c*) M. E. Stewart, C. R. Anderton, L. B. Thompson, J. Maria, S. K. Gray, J. A. Rogers and R. G. Nuzzo, *Chem. Rev.*, 2008, **108**, 494–521.

2 (*a*) D. K. Lim, K. S. Jeon, H. M. Kim, J. M. Nam and Y. D. Suh, *Nat. Mater.*, 2010, **9**, 60–67; (*b*) A. Lee, G. F. S. Andrade, A. Ahmed, M. L. Souza, N. Coombs, E. Tumarkin, K. Liu, R. Gordon, A. G. Brolo and E. Kumacheva, *J. Am. Chem. Soc.*, 2011, **133**, 7563–7570; (*c*) M. Moskovits, *Nature*, 2010, **464**, 357.

3 (*a*) M. S. Schmidt, J. Hübner and A. Boisen, *Adv. Mater*, 2012, **24**, 11–18; (*b*) R. H. Que, M. W. Shao, S. J. Zhuo, C. Y. Wen, S. D. Wang and S. T. Lee, *Adv. Funct. Mater.*, 2011, **21**, 3337–3343; (*c*) A. Kim, F. S. Ou, D. A. A. Ohlberg, M. Hu, R. S. Williams and Z. Y. Li, *J. Am. Chem. Soc.*, 2011, **133**, 8234–8239; (*d*) H. B. Tang, G. W. Meng, Q. Huang, Z. Zhang, Z. L. Huang and C. H. Zhu, *Adv. Funct. Mater.*, 2012, **22**, 218–224.

4 (*a*) Y. Fang, N. H. Seong and D. D. Dlott, *Science*, 2008, **321**, 388–392; (*b*) N. P. W. Pieczonka and R. F. Aroca, *Chem. Soc. Rev.*, 2008, **37**, 946–954; (*c*) D. K. Lim, K. S. Jeon, H. M. Kim, J. M. Nam and Y. D. Suh, *Nat. Mater.*, 2010, **9**, 60–67; (*d*) S. Z. Li, M. L. Pedano, S. H. Chang, C. A. Mirkin and G. C. Schatz, *Nano Lett.*, 2010, **10**, 1722–1727; (*e*) L. Polavarapu and L. M. Liz-Marzán, *Phys. Chem. Chem. Phys.*, 2013, **15**, 5288–5300; (*f*) L. B. Yang, P. Li, H. L. Liu, X. H. Tang and J. H. Liu, *Chem. Soc. Rev.*, 2015, DOI: 10.1039/C4CS00509K.

5 W. Dickson, G. A. Wurtz, P. R. Evans, R. J. Pollard and A. V. Zayats, *Nano Lett.*, 2008, **8**, 281–286.

6 H. L. Chen, K. C. Hsieh, C. H. Lin and S. H. Chen, *Nanotechnology*, 2008, **19**, 435304–435309.

7 (*a*) G. Xu, Y. Chen, M. Tazawa and P. Jin, *J. Phys. Chem. B*, 2006, **110**, 2051–2056; (*b*) G. Xu, C. M. Huang, M. Tazawa, P. Jin and D. M. Chen, *J. Appl. Phys.*, 2008, **104**, 053102–053110.

8 (*a*) S. Olcum, A. Kocabas, G. Ertas, A. Atalar and A. Aydinli, *Opt. Express*, 2009, **17**, 8542–8547; (*b*) K. D. Alexander, K. Skinner, S. Zhang, H. Wei and R. Lopez, *Nano Lett.*, 2010, **10**, 4488–4493.

9 (*a*) H. B. Zhou, Z. P. Zhang, C. L. Jiang, G. J. Guan, K. Zhang, Q. S. Mei, R. Y. Liu and S. H. Wang, *Anal. Chem.*, 2011, **83**, 6913–6917; (*b*) H. L. Liu, Y. D. Sun, Z. Jin, L. B. Yang and J. H. Liu, *Chem. Sci.*, 2013, **4**, 3490–3496.

10 (*a*) M. Cerruti, J. Jaworski, D. Raorane, C. Zueger, J. Varadarajan, C. Carraro, S. W. Lee, R. Maboudian and A. Majumdar, *Anal. Chem.*, 2009, **81**, 4192–4199; (*b*) M. Riskin, R. T. Vered, T. Bourenko, E. Granot and I. Willner, *J. Am. Chem. Soc.*, 2005, **127**, 6744–6751.

11 (*a*) A. G. Dong, J. Chen, P. M. Vora, J. M. Kikkawa and C. B. Murray, *Nature*, 2010, **466**, 474–477; (*b*) A. M. Smith and S. M. Nie, *Acc. Chem. Res.*, 2010, **43**, 190–200; (*c*) X. G. Peng, *Acc. Chem. Res.*, 2010, **43**, 1387–1395.

12 (*a*) K. A. Willets and R. P. Van Duyne, *Annu. Rev. Phys. Chem.*, 2007, **58**, 267–297; (*b*) J. Kneipp, H. Kneipp and K. Kneipp, *Chem. Soc. Rev.*, 2008, **37**, 1052–1060.

13 R. S. Golightly, W. E. Doering and M. J. Natan, *J. Am. Chem. Soc. Nano*, 2009, **3**, 2859–2869.

14 (*a*) W. Y. Li, P. H. C. Camargo, X. M. Lu and Y. N. Xia, *Nano Lett.*, 2009, **9**, 485–490; (*b*) B. H. Zhang, H. S. Wang, L. H. Lu, K. L. Ai, G. Zhang and X. L. Cheng, *Adv. Funct. Mater.*, 2008, **18**, 2348–2355.

15 (*a*) H. B. Zhou, Z. P. Zhang, C. L. Jiang, G. J. Guan, K. Zhang, Q. S. Mei, R. Y. Liu and S. H. Wang, *Anal. Chem.*, 2011, **83**, 6913–6917; (*b*) H. L. Liu, Y. D. Sun, Z. Jin, L. B. Yang and J. H. Liu, *Chem. Sci.*, 2013, **4**, 3490–3496; (*c*) L. B. Yang, H. L. Liu, J. Wang, F. Zhou, Z. Q. Tian and J. H. Liu, *Chem. Commun.*, 2011, **47**, 3583–3585; (*d*) K. Qian, L. B. Yang, Z. Y. Li and J. H. Liu, *J. Raman Spectrosc.*, 2013, **44**, 21–28.

16 (*a*) P. Taladriz-Blanco, N. J. Buurma, L. Rodriguez-Lorenzo, J. Pérez-Juste, L. M. Liz-Marzán and P. Hervés, *J. Mater. Chem.*, 2011, **21**, 16880–16887; (*b*) T. Demeritte, R. Kanchanapally, Z. Fan, A. K. Singh, D. Senapati, M. Dubey, E. Zakarb and P. C. Ray, *Analyst*, 2012, **137**, 5041–5045.

17 (*a*) M. S. Goh and M. Pumera, *Anal. Bioanal. Chem.*, 2011, **399**, 127–131; (*b*) S. W. Thomas III, G. D. Joly and T. M. Swager, *Chem. Rev.*, 2007, **107**, 1339–1386; (*c*) M. Riskin, R. Tel-Vered, O. Lioubashevski and I. Willner, *J. Am. Chem. Soc.*, 2009, **131**, 7368–7378; (*d*) C. J. McHugh, A. R. Kennedy, W. E. Smith and D. Graham, *Analyst*, 2007, **132**, 986–988.

18 (*a*) M. M. Liu and W. Chen, *Biosens. Bioelectron.*, 2013, **46**, 68–73; (*b*) X. He, H. Wang, Z. B. Li, D. Chen and Q. Zhang, *Phys. Chem. Chem. Phys.*, 2014, **16**, 14706–14712; (*c*) H. L. Liu, D. Y. Lin, Y. D. Sun, L. B. Yang and J. H. Liu, *Chem. – Eur. J.*, 2013, **19**, 8789–8796; (*d*) X. Zhou, H. L. Liu, L. B. Yang and J. H. Liu, *Analyst*, 2013, **138**, 1858–1864.

19 X. M. Zhao, B. H. Zhang, K. L. Ai, G. Zhang, L. Y. Cao, X. J. Liu, H. M. Sun, H. S. Wang and L. H. Lu, *J. Mater. Chem.*, 2009, **19**, 5547–5553.

20 C. Ruan, G. Eres, W. Wang, Z. Zhang and B. Gu, *Langmuir*, 2007, **23**, 5757–5760.

21 (*a*) L. B. Yang, L. Ma, G. Y. Chen, J. H. Liu and Z. Q. Tian, *Chem. – Eur. J.*, 2010, **16**, 12683–12693; (*b*) Y. R. Fang, Y. Z. Li, H. X. Xu and M. T. Sun, *Langmuir*, 2010, **26**, 7737–7746; (*c*) K. A. Mahmoud and M. Zourob, *Analyst*, 2013, **138**, 2712–2719.

22 A saturated solution of TNT in ethanol was made. 1 ml of TNT solution was deposited onto wad of wool, which was inserted into a long copper pipe with 100 mL volume. The pipe was inserted into the heater, which contained 60 °C such that the two ends of the pipe protruded. Through fixtures nitrogen carrier gas was blown through the heated pipe. The nitrogen gas at the exit of the heated pipe was assumed to be saturated with TNT.